Exploring the Effect of Contact Location on FSR and Piezoelectric Sensor Outputs to Transduce Slowly- and Rapidly Adapting Tactile Feedback for Sensory Prostheses

Sharon Wong

Dr. Dustin Tyler Lab | Summer 2023

Introduction

The sense of touch is an essential aspect of human perception, facilitating interaction with our surroundings [1]. As humans increasingly interface with environments via robotic devices, including prostheses and other robotic manipulators, the ability to mimic the intricate and delicate movements of a human hand becomes increasingly desirable [2]. Despite the development of high degree-of-freedom (DOF) robotic devices, achieving precise and intuitive control remains a significant challenge, particularly due to a lack of sensory feedback [3], [4].

Natively, the sense of touch is elicited by two classes of mechanoreceptors: slowly-adapting (SA), which detects sustained pressure on the skin and most directly mimics the stimulus, and rapidly-adapting (RA), which best detects change. Current force-sensing techniques primarily focus on slowly adapting analogs, limiting the captured information. To address this issue, our research investigates the value of two robotic sensors: Force-Sensing Resistors (FSR) and piezoelectric materials.

While FSRs are commonly employed to measure force directly, similar to an SA mechanoreceptor, their larger form factor limits the application area and measurement reliability across their surface area. Piezoelectric sensors present a smaller force-transducing alternative with the potential to capture RA-analogue information and enrich the tactile feedback relayed to the user (Figure 1).

To evaluate the sensitivity of the FSR and piezoelectric sensors across their receptive fields, we analyzed sensor performance under a range of applied weights across different contact locations. By understanding the sensor sensitivity profiles, we can determine how to apply these sensors for closed-loop control of neuroprostheses and other robotic devices.

Material and Methods

Our study aims to assess the impact of contact location on force sensor performance for both the slowly-adapting sensor (FSR) and the rapidly-adapting sensor (piezoelectric).
Introducing the Interlink Electronics Sensor Technologies FSR 402 with a force range of 30g to 1000g, expertly paired with a 10k ohms resistance [5]. These FSRs operate as two-wire devices, adjusting their resistance based on the force applied to them. With a maximum voltage of 5V, they offer exceptional performance and precision in various applications. Based on equation1, we knew that when force applied the voltage increase while the resistance decrease.

$$V_{out} = \frac{R_M V}{(R_M + R_{FSR})} \qquad (1)$$

On the other hands, presenting the muRata Piezoelectric Film Sensor (Picoleaf™) with a maximum voltage capacity of 3.3V [6]. The output signal of this sensor falls within the range of -512 to +512. It's worth highlighting that the output value of the piezoelectric sensor is obtained by the applied force dividing by time. Later on, we'll delve into integrating the output readings over time to derive the corresponding voltage measurement.

We tested a variety of location-weight combinations for each sensor, five trials per condition. Locations were spaced 0.25 cm apart along the central longitudinal axis of each sensor, yielding five (Figure 1) and

three (Figure 2) distinct locations for the FSR and piezoelectric sensors, respectively, due to their different sizes.

Fig1: FSR with Contact Locations

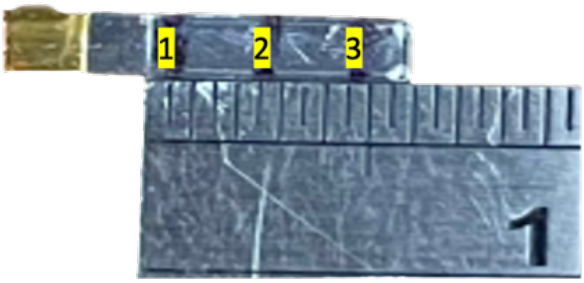

Fig2: Piezoelectric with Contact Locations

Hardware Setup

The platform apparatus was designed using Onshape and 3D-printed. A pin protrudes from the bottom of the platform to allow precise force application to specific sensor locations when masses are placed on the platform. Concentric rings in the platform surface secure various mass sizes.

Fig3(a)

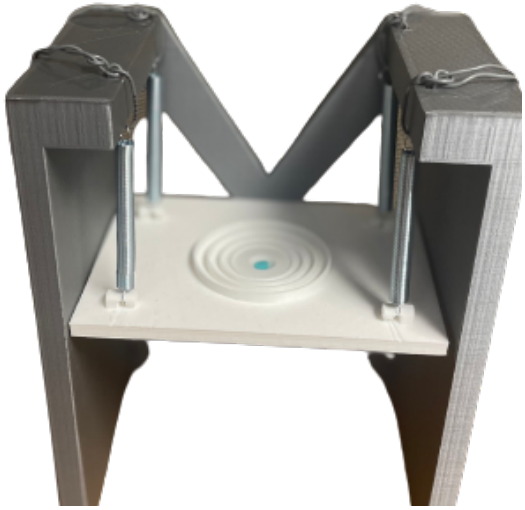

Fig3(b)

Fig3: 3D-printed Design. 3D print for heavyweight experiments. (a) Front view (b) Bottom view.

Software Setup

The software requirements for both sensory setups are different and will be listed in this section

FSR software setup:

To update your code from Arduino to Sparkfun ESP32 and transition from using the Arduino Serial Monitor to CoolTerm, first, ensure your code is compatible with the Sparkfun ESP32 platform. Next, close the Arduino IDE, as it will no longer be used for this project. Download CoolTerm, a terminal emulator that will serve as the new communication interface for the Sparkfun ESP32. In CoolTerm, configure the platform settings by changing the communication port to USB, which connects to the Sparkfun ESP32, and adjusting the Baudrate rate to 9600, the required data transmission speed for your setup.

Before establishing the connection with the Sparkfun ESP32 using CoolTerm, double-check that you have closed the Arduino IDE to prevent any potential conflicts or issues. Once properly set up, you can now communicate with the Sparkfun ESP32 through CoolTerm and receive the data it transmits. To store the received data for future analysis, instruct CoolTerm to log the data into a .csv file.

Piezoelectric software setup:

To utilize the USB oscilloscope on your Microsoft 10 laptop, you need to follow these steps. First, download the USB oscilloscope executable files. Afterward, create a folder specifically labeled "Oscilloscope" and place the necessary .dll and .ini files inside it. Once done, put the "Oscilloscope" folder and the .exe file together in the same directory. This arrangement will ensure smooth functionality when running the USB oscilloscope application.

Next, you should modify the Baudrate rate to 9600 for optimal performance. Additionally, open Channel 1 and 2 to enable data acquisition from both channels. Finally, ensure that you save the collected data in .csv format for convenient storage and analysis.

Procedure

Masses were applied to specific points either via Von Frey filaments for lower weights or a spring-suspended platform for larger masses (Figure 4). We obtained the per-location sensor output curves by applying a range of applied weights at each location. Von Frey filaments were applied directly for 4g, 6g, 8g, 10g, 15g, 26g, 30g, 60g, 100g, and 180g masses. The 3D-printed apparatus was used for masses of 200g, 500g, and 1000g. The force applied to the sensor via the spring-mass system was computed as $F_{sensor} = F_{platform} + F_{mass} - F_{springs}$, where $F_{platform}$ and F_{mass} are computed using $F=m*g$ and $F_{springs} = 4 * k_{spring} * \Delta x_{spring}$. Also, there are two springs one is SP 9601 max load: of j1.39lbs, shorter, thicker spring, and another is SP 9607 max load: 0.9lbs, longer, skinnier spring.

The FSR and piezoelectric sensors were tested over 30g-1000g and 4g-200g ranges, respectively.

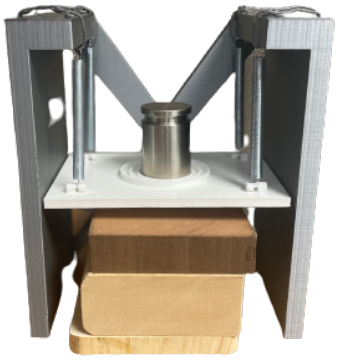

Fig4: Hardware setup

Data analyzed

We investigated data through Python from both sensors, using various statistical analyses.

FSR data analyzed:

To analyze the data from different files, follow these steps. First, place the data file.csv and data.py script in the same folder. Then, execute the data.py script to perform the analysis. You can run the script using the following command in Python 3:
python3 data.py -i filename filename filename filename filename filename > output_filename.dat

For examples:

python3 data.py -i 60g_1-1 60g_1-2 60g_1-3 60g_1-4 60g_1-5 > 60g_1.dat

After running the code, we separated all the values greater than zero and computed the average for each file. Additionally, the averages of five files and the overall average of these five files' averages are recorded in the .dat files (Figure 6). The figure illustrates all five files' values that are greater than zero (Figure 5).

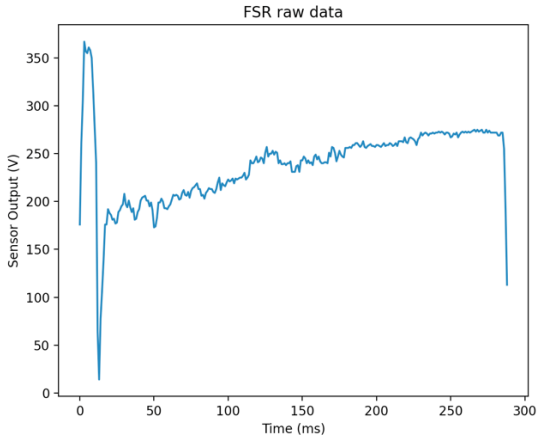

Fig5: FSR non-zero Raw Data

```
The average of non-zero numbers in 60g_1-1 is: 331.28228228228227
The average of non-zero numbers in 60g_1-2 is: 375.4095744680851
The average of non-zero numbers in 60g_1-3 is: 419.37444933920705
The average of non-zero numbers in 60g_1-4 is: 230.93684210526317
The average of non-zero numbers in 60g_1-5 is: 238.03114186851212

The overall average of the averages from the five files is: 319.00685801266997
```

Fig6: FSR dat file

If you wish to analyze a different number of files, you can adjust the script on line 5 by changing the 'nargs' value in the argument parser. After running the analysis, you can read the data from the generated .dat file for further examination and interpretation. By following these steps, you can efficiently analyze multiple data files using Python and gain valuable insights from the processed data.

Piezoelectric data analyzed:

To begin the data analysis process, place the .csv data file and piedata.py in the same folder. Next, execute the "piedata.py" script to initiate the analysis. You can run the script using the following command in Python 3:

python3 piedata.py -i filename.csv > output_filename.dat

For example:

python3 piedata.py -i 100g_1-1.csv > 100g.dat

Once the analysis is complete, you can proceed to read the data from the generated .dat file. In the initial findings, focus on identifying the range in the Integrated Data figure (Figure 8). Subsequently, examine the .dat file (Figure 9) to identify the plateau numbers. These plateaus are essential for understanding specific patterns or trends within the data and can provide valuable insights for further analysis and interpretation. By following these steps, you can effectively analyze the data from which we integrated the output readings over time for the piezoelectric sensor to account for the output signal peak and width.

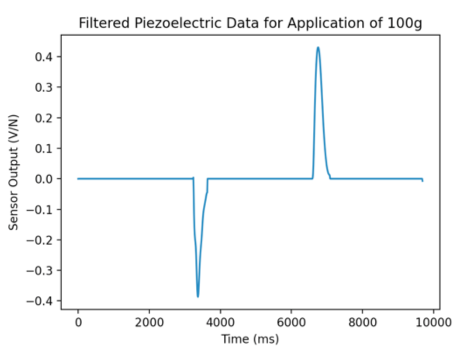

Fig7: Piezoelectric Spike Data

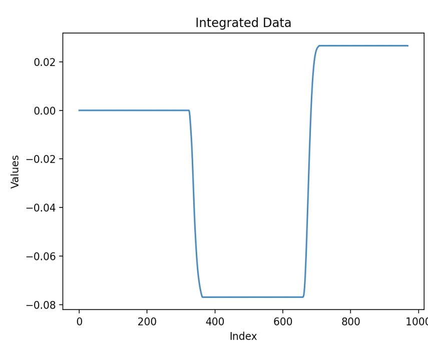

Fig8: Piezoelectric Integrated Data

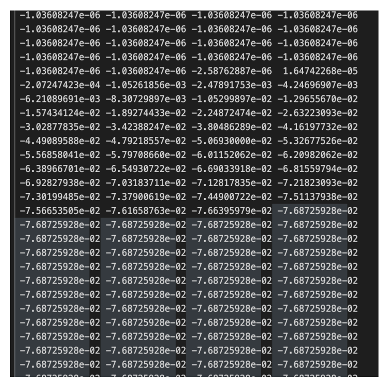

Fig9: Piezoelectric dat file

Results

Based on the obtained force-output curves (Figure 10), we selected the range for FSR before 2N, which had the liner portion, and for the Piezoelectric range before 1N due to after 1N, it stated decreased. Thus, the overlap masses are 60g and 100g for analysis.

Fig10(a) Fig10(b)

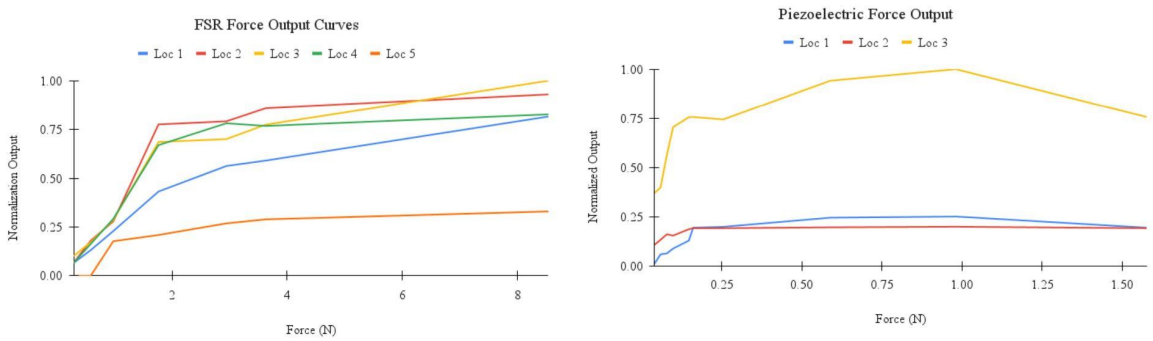

Fig10: Force-Output Curves. The FSR and piezoelectric sensors were tested over 30g-1000g and 4g-200g ranges, respectively. Each color represents a different contact location (see Figs. 3-4). (a) The output of an FSR sensor decreases as the contact location on the sensor moves further away from the sensor's center. (b) The output of a piezoelectric sensor increases at the most distal location.

First, we assessed the stability of each sensor output across contact locations. For both sensors, ANOVA and Tukey's HSD tests showed significant differences between at least one pair of the tested locations. The FSR sensor was more sensitive at central locations compared to the first and last locations (Figure 11). At 60g on the FSR, the most distal location (Loc5) returned no output and thus was significantly different from all the other locations ($p<0.001$, Fig11a). At 100g, location 5 significantly differed from locations 2-4 ($p<0.01$, Fig11b). Overall, only the most distal location had a consistently different sensitivity on the FSR receptive field.

The piezoelectric sensor was most sensitive distally (Loc3). At 60g, only location 3 showed a significant difference ($p<0.001$, Fig11c). At 100g, location 3 was still significantly different from locations 1-2 ($p<0.001$), but locations 1-2 were also significantly different ($p<0.05$, Fig11d). Overall, the location had a significant effect on the piezoelectric sensor output, indicating low sensor stability across its receptive field.

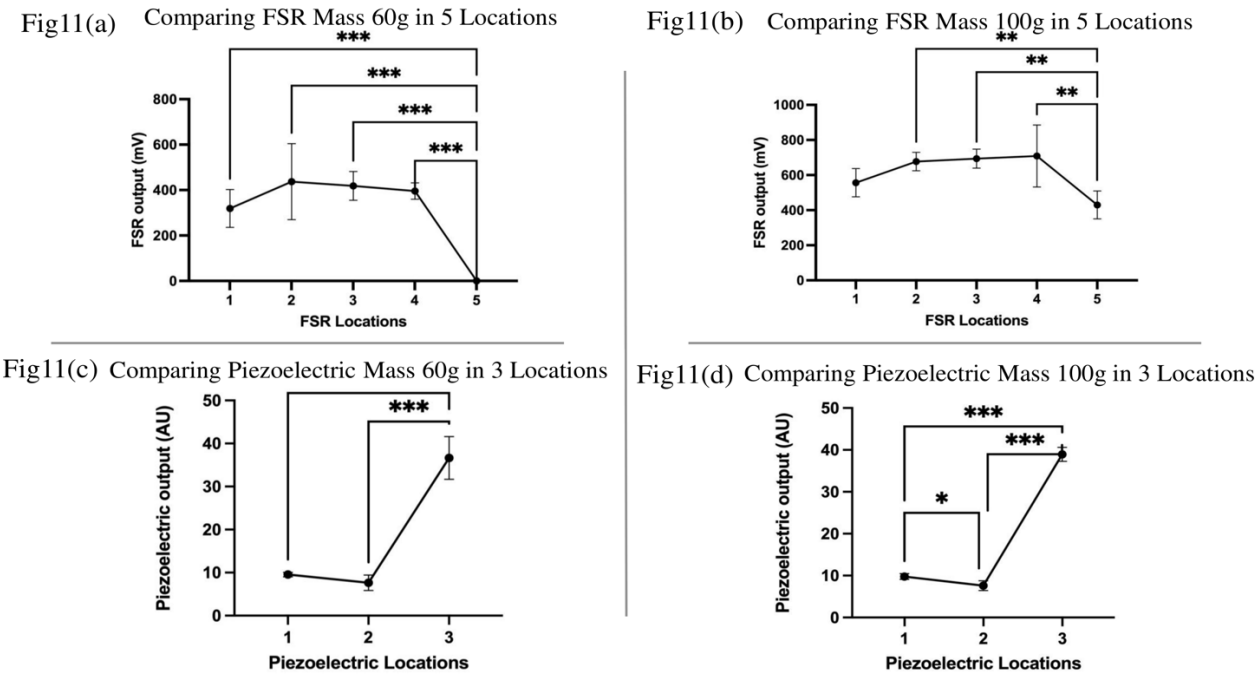

Fig11: Force Sensor Outputs across Contact Locations Analyzed by ANOVA and Tukey HDS. (a) At 60g on the FSR, the most distal location (Loc5) returned no output and thus was significantly different from all the other locations ($p<0.001$). (b) At 100g on the FSR, location 5 was significantly different from only locations 2-4 ($p<0.01$). (c) At 60g on the piezoelectric, only location 3 showed a significant difference ($p<0.001$). (d) At 100g on the piezoelectric, location 3 was still significantly different from locations 1-2 ($p<0.001$), and locations 1-2 were also significantly different ($p<0.05$).

Second, we investigated the sensitivity of each sensor to different masses (Figure1). The FSR exhibited a significant difference between 60g and 100g ($p<0.01$), highlighting its ability to discriminate between different masses. The piezoelectric sensor outputs were not statistically different between the two masses.

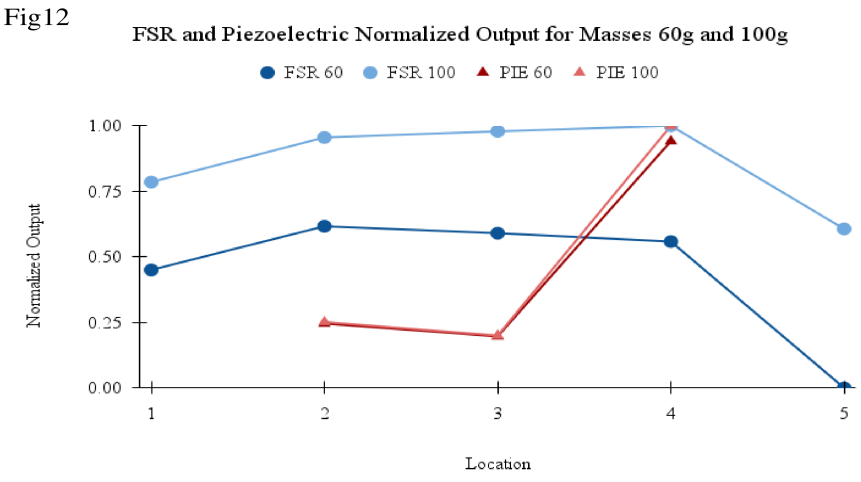

Fig12: FSR and Piezoelectric Normalized Output for Masses 60g and 100g.
The FSR exhibited a significant difference in output between 60g and 100g ($p<0.01$).

Discussion

These findings indicate FSRs provide more stable measurements across their receptive field compared to piezoelectric, suggesting continued FSR use for primary force transduction. However, the location-influenced activation of both sensors still limits their receptive fields to smaller areas than their physical form factors, and additional sensors should be considered in the future.

Additionally, FSRs better discriminate between different forces applied. The piezoelectric's low sensitivity to different masses suggests its suitability for tactile submodalities like RA edge detection, saving SA continuous monitoring for FSRs.

Conclusion

Throughout our experiments, we examined two force sensors, subjecting them to varying forces at different locations. The results revealed that FSR sensors exhibit higher stability across locations and are more sensitive to force variations compared to piezoelectric sensors. FSRs offer a continuous touch representation akin to SA fibers, while piezoelectric sensors exhibit behavior similar to RA fibers. This research provides valuable insights into the capabilities and optimal applications of these two sensors for artificial tactile sensation.

For future directions, our research underscores the continued suitability of FSRs for primary force transduction in various applications. To ensure accurate sensory feedback, it will be crucial to minimize the impact of location-influenced activation. Thus, we propose enhancing the sensory feedback system by incorporating both direct force transduction and edge detection to closely resemble real-world touch sensations.

Furthermore, our aim is to compare the original force sensor used in the TASAK robotic hand with the findings from our research. This comparison will enable us to gain a comprehensive understanding of the performance and advantages of these sensors, we can enrich the sensation and perception of environments through human-robot interfaces, ultimately improving the overall interaction between humans and robots.

Reference

[1] Jenkins, B. A., & Lumpkin, E. A. (2017). Developing a sense of touch. Development, 144(22), 4078–4090. https://doi.org/10.1242/dev.120402

[2]Sihombing, P., Muhammad, R. B., Herriyance, H., & Elviwani, E. (2020). Robotic arm control based on fingers and hand gesture. 2020 3rd International Conference on Mechanical, Electronics, Computer, and Industrial Technology (MECnIT). https://doi.org/10.1109/mecnit48290.2020.9166592

[3] F. Amirabdollahian et al., “Prevalence of haptic feedback in robot-mediated surgery: a systematic review of literature,” J. Robot. Surg., vol. 12, no. 1, pp. 11–25, 2018, doi: 10.1007/s11701-017-0763-4.

[4] M. K. Chmarra, J. Dankelman, J. J. van den Dobbelsteen, and F.-W. Jansen, “Force feedback and basic laparoscopic skills,” Surg. Endosc., vol. 22, no. 10, pp. 2140–2148, 2008, doi: 10.1007/s00464-008-9937-5

[5] FSR Model 402. Interlink Electronics Shop. (n.d.). https://buyinterlinkelectronics.com/collections/new-standard-force-sensors/products/fsr-model-402

[6] Piezoelectric Film Sensor (picoleafTM). Murata Manufacturing Co., Ltd. (n.d.). https://www.murata.com/en-us/products/sensor/picoleaf